Int Nano Lett (2017) 7:43–49
DOI 10.1007/s40089-017-0200-8

ORIGINAL ARTICLE

Study of conversion of butadiene to CO_2 by $rTiO_2$ nanoparticles: ZINDO/S

Leila Mahdavian[1]

Received: 9 August 2015 / Accepted: 1 February 2017 / Published online: 17 February 2017

Abstract One of the pollutants emitted from automobile exhaust is unburned hydrocarbons that include benzene, propane, formaldehyde, butadiene, etc. Due to the carcinogenicity of these substances, eliminating and reducing them in the source of production is essential. Catalytic converters have been developed to reduce these pollutions to low-risk materials in automobile exhaust. In this study, the mechanism of converting butadiene to carbon dioxide is simulated and calculated by rutile titanium dioxide (Titania) nanoparticles ($rTiO_2$-NP). Then the geometric structure of simulated steps (the conversion butadiene to carbon dioxide) is optimized by DFT method and semi-empirical (ZINDO/S) method is used to calculate the thermodynamic properties. There are three different locations of physical chemistry on the $rTiO_2$-NPs to get closer pollutants, namely Ti–O (1), Ti–O (2), and Ti–Ti. The results show the approaching possibility of butadiene to Ti–O (1) is more than other locations, because the bond length, electronegativity and spatial structure of this position are different from others.

Keywords Butadiene · $rTiO_2$-NP · Unburned hydrocarbons · Nanocatalyst · DFT · ZINDO/S

Introduction

The motor vehicles pollute the air more than any other activity of human [1–4]. By regular inspection and repair of engines and using clean fuel, entry of pollutants into the environment can be decreased [5, 6]. The gases released by vehicles included unburned hydrocarbons, carbon monoxide and nitrogen oxides [7, 8]. There are many ways to get better fuel burning. The main source of unburned hydrocarbon emissions from the automobile exhaust is the design of the combustion chamber. For better burning, fuel should have more contact with the combustion chamber wall, so the surface of the combustion chamber walls should be minimized as possible; for this, the chamber should be of spherical shape but practically it is not possible [9–11]. Hydrocarbons in the fuel are composed of 20 species and 100 subspecies, of which the majority of them are in the exhaust gases, e.g., benzopyrene, formaldehyde, butadiene, etc. [12].

The aim of this study is an evaluation of low-cost methods that can reduce many of these pollutants. Using suitable nano-filters in the exhaust of an automobile can be converted unburned hydrocarbons to low-risk compounds [13–16]. The titanium dioxide is include photo-chemistry material of the semiconductor and nano-magnets. TiO_2 (titania) has some unique characteristics such as photo-physical and photocatalysts, if their dimensions are nanoscale, these features will appear. Because of smaller dimensions of semiconductor particles, there is increased number of atoms located on the surface, and increased surface to volume ratio. This gives greater access to active sites and is increasing the amount of electrical charge carrier transfer [17].

Therefore, the interaction of rutile titanium dioxide nanoparticles ($rTiO_2$-NP) and butadiene is simulated by software GaussView 5.0.

Butadiene interaction on different places of rutile titanium dioxide nanoparticles is simulated and is optimized. The geometric structures of converting them to low-risk products are calculated. Figure 1 is a model of the ball and

✉ Leila Mahdavian
Mahdavian_leila@yahoo.com; Mahdavian@iau-doroud.ac.ir

[1] Department of Chemistry, Doroud Branch, Islamic Azad University, P.O. Box: 133, Doroud, Iran

spring for rutile titanium dioxide nanoparticles (rTiO$_2$-NP), which shows the two views and another size for it [rutile TiO$_2$ (110) nano-surface] [18, 19]. In this study, rutile titanium dioxide nanoparticles (rTiO$_2$-NP) are used, the pollutants close to the cross bridges of Ti–O (1), Ti–O (2) and Ti–Ti on rTiO$_2$-NP and the thermodynamic properties were evaluated by semi-empirical (ZINDO/S) method [20, 21].

Computational methods

Basically, the behavior of titanium dioxide photocatalysts is dependent on the electrical structure and its dimensions. A nano-material may have a different behavior which is determined using electrical structure, quantum size and the effects of the surface [22]. The electronic structure design is important based on changes in the composition and physical structure. For this purpose, the thermodynamic and electrical properties of chemical process are calculated semi-empirically; the ZINDO/S method is widely used to calculate the heat of formation, the geometry of the molecule, ionization energy, electron continuity, and other features [23]. The geometric structures are optimized by the DFT because the results could be obtained with a better accuracy [24, 25].

Rutile is a body-centered tetragonal unit cell, with unit cell parameters $a = b = 4.584$ Å, and $c = 2.953$ Å. The titanium cations have a coordination number of 6 meaning they are surrounded byQuery an octahedron of 6 oxygen atoms. The oxygen anions have a coordination number of 3, they result in a trigonal planar coordinated structure. The rutile also shows a screw axis when its octahedra is viewed sequentially [26]. This k-point grid constrained the total energy within 0.01 eV Å^{-1}/atom and the diagonal elements of the response matrix within 1%. However, convergence of the final results was not achieved, due to numerical instability of the inversion of a near-singular matrix. A cutoff of 500 eV, and k-point mesh of $4 \times 4 \times 6$, centered on the Γ point, was found to be sufficient for rutile TiO$_2$-NP [27].

In this study is calculated and studied the approaching pollutants to Ti–O bond (the first and second probability are two different locations of Ti–O on rTiO$_2$-NP and the third probability is Ti–Ti bond) (Fig. 2). So geometrical structures of them are optimized by B3LYP/6-31G. Their thermodynamic properties are assessed by the ZINDO/S in semi-empirical method.

Results and discussion

The Z-matrix files write for titanium dioxide nanoparticles structure (angles and length of bonds between oxygen and titanium) by experimental data of X-ray diffraction (Fig. 1) [28], then Z-matrix files are optimized by the B3LYP method with 6-31G-based set on the GAMESS program package under Linux [29]. Oxidation of butadiene into carbon dioxide and oxygen is:

$$C_4H_6 + r\mathrm{TiO_2} - \mathrm{NP} \rightarrow C_4H_4 - r\mathrm{TiO_2} - \mathrm{NP} + H_2$$

$$C_4H_4 - r\mathrm{TiO_2} - \mathrm{NP} + 2H_2 \rightarrow 2C_2H_4 + r\mathrm{TiO_2} - \mathrm{NP}$$

$$2C_2H_4 - r\mathrm{TiO_2} - \mathrm{NP} + 4O_2 \rightarrow 4CO_2 + 4H_2 + r\mathrm{TiO_2} - \mathrm{NP}$$

Pollutants near the outside surface of TiO$_2$ (titania) nanostructure and are bonded to the surface and electron exchange takes place between them, then the pollutants are converted to carbon dioxide. Figure 3 shows all steps of the simulation for butadiene interaction to CO_2 and H_2.

In this study, the interaction of butadiene with rTiO$_2$ nanoparticles have been simulated in nine steps (Fig. 3); from first and second steps butadiene is closed in rTiO$_2$-NPs, then in the third step, transition state of conversion of butadiene to ethylene occurs, in the fourth step product

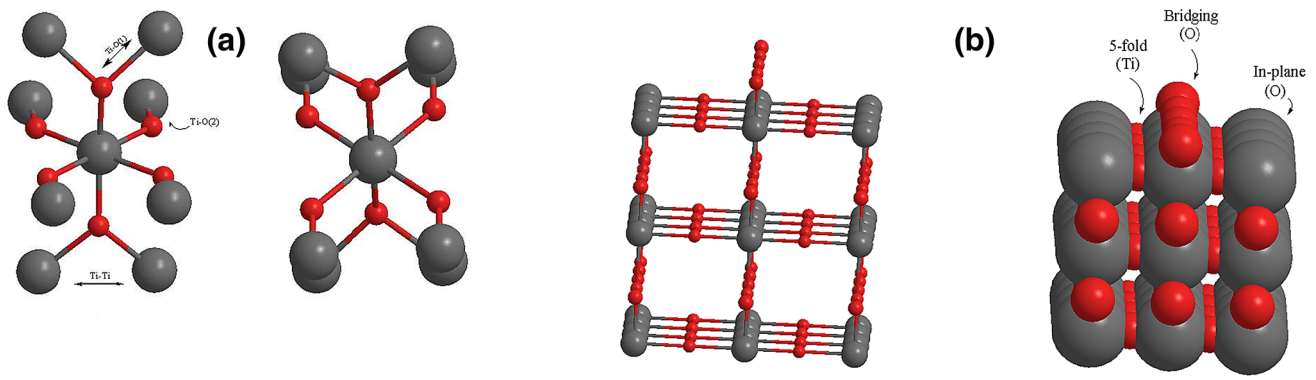

Fig. 1 Ball-and-stick model configuration of **a** rutile TiO$_2$ nanoparticle front view (to specify the location of *three*) and *top view*, **b** rutile TiO$_2$ (110) nano-surface

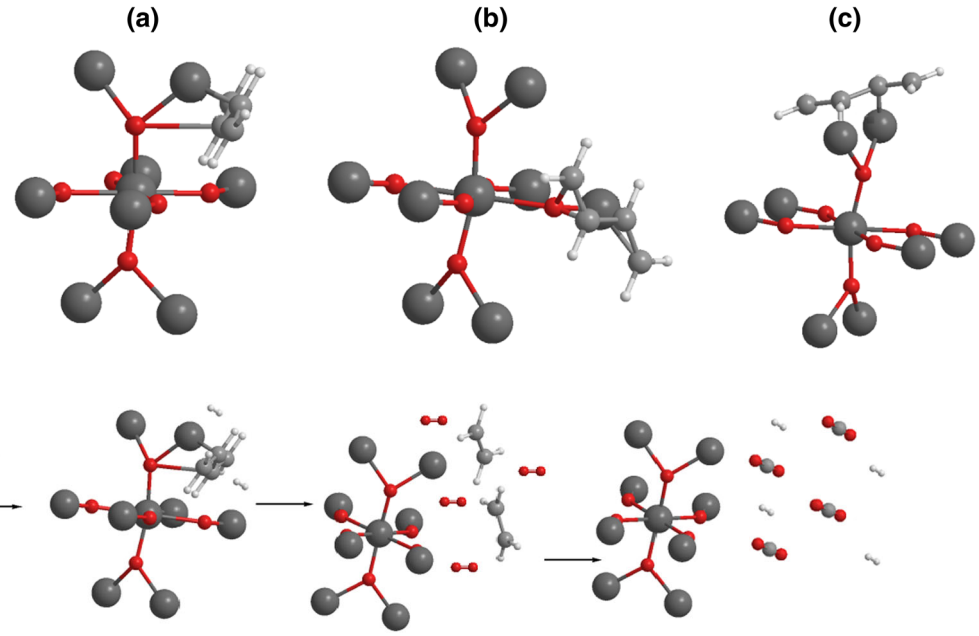

Fig. 2 Probability of butadiene interaction with different location of rTiO$_2$-NP; **a** Ti–O (1), **b** Ti–O (2) and **c** Ti–Ti

Fig. 3 Ball-and-stick model configuration of butadiene interaction on cross bridge of Ti–O in rutile TiO$_2$ nanoparticle

generated from the surface is removed. In fifth and sixth steps, the ethylene molecules are closed on the surface and in the seventh and eight step transition state conversion of them to CO_2 and H_2, respectively. Then conversion was completed in ninth step and CO_2 molecules are produced, then it is excreted from rTiO$_2$-NPs. The electronic structure and the thermodynamic properties are calculated for all steps by ZINDO/S-DFT.

The thermodynamic properties of these interactions on Ti–O and Ti–Ti cross bridges are shown in Tables 1, 2, and 3. All thermodynamic properties are shown in the table except that the dipole moment and RMS gradient are obtained by the following equation:

$$\begin{aligned} E_{T_{\text{initial}}} &= E_{T_{(\text{cleansurface})}} + E_{T_{(\text{molecule})}} \\ E_{T_{\text{final}}} &= E_{T_{(\text{surfacewithmolecule})}} \\ E_{\text{ads}} &= \Delta E_T = E_{T_{\text{final}}} - E_{T_{\text{initial}}}. \end{aligned} \tag{1}$$

From Fig. 4 and Tables 1, 2, and 3, the lowest energy is in the final product (CO_2), which shows molecules of carbon dioxide are more stable than butadiene molecules. In third and sixth steps, a sudden change in energy and other thermodynamic parameters calculated is observed. For the intermediate to product, this sudden change in energy can be seen in seventh and eighth steps.

The third step is transitioning state of butadiene to ethylene molecules. The sixth step is transitioning state of ethylene to CO_2. Dipole moments for all steps are calculated and are shown in Tables 1, 2, and 3, most changes of which are in the transition state of intermediates (third and sixth steps).

As the results show, from comparisons of data in Tables 1, 2 and 3, the probability of pollutant interaction on cross bridge of Ti–O (2) is more than other locations. The distance of Ti–O (1), Ti–O (2) and Ti–Ti bonds are equal to 2.02, 1.62 and 2.95 Å, respectively (Fig. 5). The electronegativity difference ($\Delta\chi$) of Ti–O and Ti–Ti are 2.90 and 0. The bond number of Ti–O is more in the structure of rTiO$_2$-NP and space inhibited of Ti–O is also less than Ti–Ti. Bond length of Ti–O (2) is closer to the bond lengths of C=C and C–C in butadiene (Fig. 5).

To access to the electrical properties these interactions are used the electrical energy and it is obtained from the following equation [30]:

$$E_{\text{elec}} = RI, \tag{2}$$

where R is the electrical resistance and I is the current intensity per (A), that I can be found from $I = \frac{q}{t}$ yielding the following equation:

$$R = \frac{E_{\text{elec}} t}{nF}. \tag{3}$$

The electrical resistance of all steps and conversions are computed based on electrical data, Eqs. (2) and (3), as can be seen in Fig. 6. The electrical resistance of Ti–O bonds is different from Ti–Ti for the second to seventh steps, but for all bonds in the transition state of intermediate, the electrical resistance increases, the electrical resistance of CO_2 is decreased; in these conditions increases the electrical conductivity and the electron exchange of butadiene and rTiO$_2$-NP is easier to occur than in transition state steps.

Table 1 The thermodynamic properties of butadiene interaction on Ti–O (1) cross bridge in rTiO$_2$-NP at 298 K by ZINDO/S-DFT

Cross bridge of Ti–O(1) in rutile							
	E_{total} (kcal/mol)	Dipol moment (D)	RMS (kcal/mol Å)	E_{bin} (kcal/mol)	H (kcal/mol)	G_{ele} (kcal/mol)	E_{nuc} (kcal/mol)
rTiO$_2$-NP	−67,934.53	3.81	415.1	−12,183.09	−10,815.04	−237,906.98	169,972.45
Butadiene	−16,581.28	0.0006	181.7	−3476.01	−2479.84	−39,587.18	23,005.89
Steps	ΔE_{total} (kcal/mol)	Dipol moment (D)	RMS (kcal/mol Å)	ΔE_{bin} (kcal/mol)	ΔH (kcal/mol)	ΔG_{ele} (kcal/mol)	ΔE_{nuc} (kcal/mol)
1	−26,458.97	5.44	344.0	−5577.57	−6223.88	−172,072.64	145,613.68
2	−27,619.08	12.41	356.2	−6737.68	−7384.00	−187,887.55	160,268.48
3	−28,226.18	29.17	400.1	−7344.79	−7991.10	−195,280.72	167,054.54
4	−30,119.62	10.1	359.4	−8635.87	−9177.98	−214,876.40	184,756.79
5	−28,789.34	92.87	350.0	−7305.49	−7847.60	−203,010.80	174,221.57
6	−28,678.36	9.835	340.3	−7194.61	−7736.72	−201,480.16	172,801.81
7	−18,629.06	12.93	382.5	−3999.13	−5091.42	−118,905.54	100,276.87
8	−19,487.68	5.64	394.5	−4857.75	−5950.05	−125,876.54	106,388.87
9	−83,987.85	3.08	429.0	−8596.51	−9078.97	−428,239.59	344,251.75

Table 2 The thermodynamic properties of butadiene interaction on Ti–O (2) cross bridge in rTiO$_2$-NP at 298 K by ZINDO/S-DFT

Cross bridge of Ti–O(2) in rutile							
	E_{total} (kcal/mol)	Dipol moment (D)	RMS (kcal/mol Å)	E_{bin} (kcal/mol)	H (kcal/mol)	G_{ele} (kcal/mol)	E_{nuc} (kcal/mol)
rTiO$_2$-NP	−67,934.53	3.81	415.1	−12,183.09	−10,815.04	−237,906.98	169,972.45
Butadiene	−16,581.28	0.0006	181.7	−3476.01	−2479.84	−39,587.18	23,005.89
Steps	ΔE_{total} (kcal/mol)	Dipol Moment (D)	RMS (kcal/mol Å	ΔE_{bin} (kcal/mol)	ΔH (kcal/mol)	ΔG_{ele} (kcal/mol)	ΔE_{nuc} (kcal/mol)
1	−26,232.51	4.31	342.3	−5351.12	−5997.43	−164,271.48	138,038.97
2	−27,467.56	1.59	346.1	−5986.16	−6632.48	−177,283.27	150,415.72
3	−27,589.74	3.15	360.5	−6708.35	−7354.66	−192,223.27	164,633.54
4	−29,167.95	9.74	350.8	−7684.19	−8226.30	−210,184.10	181,016.17
5	−29,217.84	12.52	350.5	−7734.09	−8276.20	−209,506.96	180,289.13
6	−27,355.74	4.36	334.0	−5871.99	−6414.10	−177,516.90	150,161.17
7	−18,382.37	5.03	364.6	−3752.43	−4844.73	−113,035.17	94,652.82
8	−19,626.32	10.20	386.4	−4996.38	−6088.68	−132,141.66	112,515.35
9	−83,987.85	3.08	429.0	−8596.51	−9078.97	−428,239.59	344,251.75

Equation constant and other thermodynamic parameters such as Gibbs free energy, enthalpy and entropy of the whole reactions were computed through the following equation:

$$K = \exp\left(-\frac{\Delta G_{ele}}{Rt}\right). \quad (4)$$

where T is the reaction temperature that is considered to be 298 K. The entropy reactions are computed by:

$$\Delta S_{ele} = \frac{\Delta H_{ele}}{T} \quad (5)$$

Other thermodynamic properties of intermediate with raw materials and intermediate with products are shown in Table 4. These data show rTiO$_2$-NP acts as photo-catalyst for the removal of pollutants in the source of production. These interactions are spontaneous and favorable. The thermodynamic parameters in Table 4 show the interaction of butadiene with the Ti–O (2) bound is more possible.

Conclusion

Anatase and rutile have the same chemical formula (TiO_2) and have same geometrical symmetry (tetragonal) but show different physicochemical properties. Titanium dioxin molecules on the metal surface are activated by

Table 3 The thermodynamic properties of butadiene interaction on Ti–Ti cross bridge in rTiO$_2$-NP at 298 K by ZINDO/S-DFT

Cross bridge of Ti–Ti in rutile							
	E_{total} (kcal/mol)	Dipol moment (D)	RMS (kcal/mol Å)	E_{bin} (kcal/mol)	H (kcal/mol)	G_{ele} (kcal/mol)	E_{nuc} (kcal/mol)
rTiO$_2$-NP	−67,934.53	3.81	415.1	−12,183.09	−10,815.04	−237,906.98	169,972.45
Butadiene	−16,581.28	0.0006	181.7	−3476.01	−2479.84	−39,587.18	23,005.89
Steps	ΔE_{total} (kcal/mol)	Dipol moment (D)	RMS (kcal/mol Å)	ΔE_{bin} (kcal/mol)	ΔH (kcal/mol)	ΔG_{ele} (kcal/mol)	ΔE_{nuc} (kcal/mol)
1	−26,814.27	8.77	348.0	−5932.87	−6579.19	−172,332.05	145,517.80
2	−27,178.88	4.35	349.0	−6297.49	−6943.80	−176,624.66	149,445.78
3	−27,676.93	4.70	359.0	−6795.54	−7441.86	−182,809.02	155,132.09
4	−29,156.8	4.72	346.0	−7673.06	−8215.17	−199,896.91	170,746.12
5	−28,840.93	9.51	348.4	−7357.18	−7899.29	−196,659.05	167,818.12
6	−28,700.85	9.29	354.3	−7217.10	−7759.20	−197,025.66	168,324.79
7	−18,932.02	2.96	374.9	−4302.08	−5394.38	−115,417.08	96,485.07
8	−19,155.24	2.83	384.1	−4525.31	−5617.60	−117,886.44	98,731.21
9	−83,987.85	3.08	429.0	−8596.51	−9078.97	−428,239.59	344,251.75

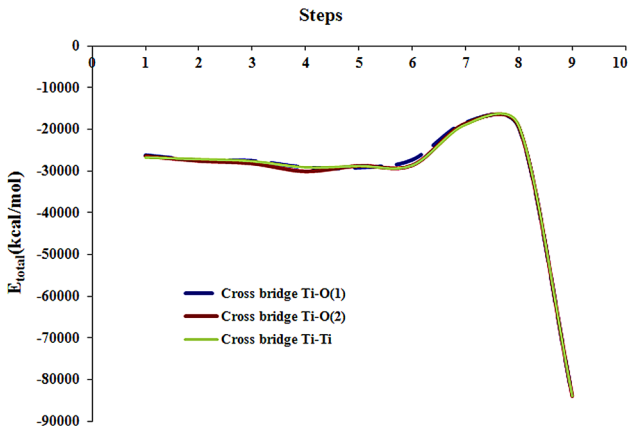

Fig. 4 The total energy of butadiene interaction on rTiO$_2$-NP by ZINDO/S method

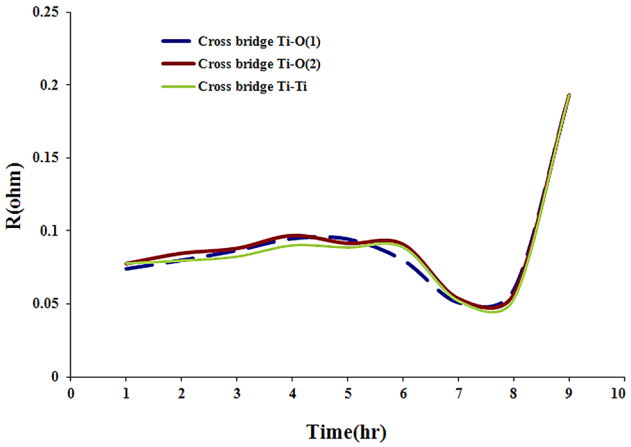

Fig. 6 The electrical resistance of butadiene interaction on rTiO$_2$-NP by ZINDO/S method

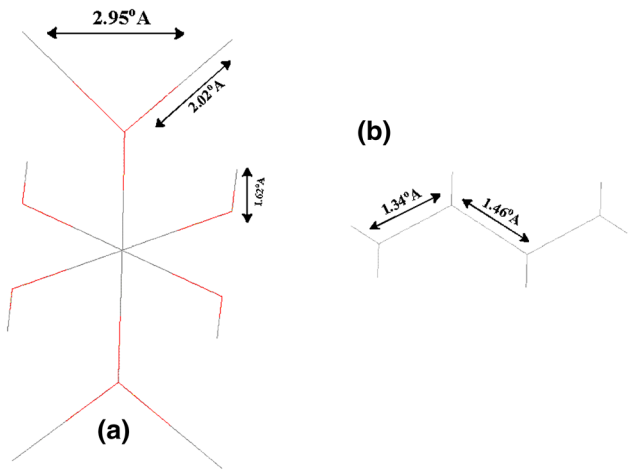

Fig. 5 The stick model configuration of rTiO$_2$-NP and butadiene with their bond length

ultraviolet radiation and during some chemical processes make bacteria, algae and fungi disappear [31]. When ultraviolet ray is radiating to titanium dioxide, the electrochemical reactions are happening and is created the production of free radicals. Free radicals are combined with pollutants and destroy them.

After attraction of the sun's ultraviolet by rTiO$_2$-NP, the electrons of capacity balances are displaced to guide band balance, and an empty hole appears in capacity balance, so the following can be considered:

$$TiO_2 + h\nu \rightarrow TiO_2\left(e^-_{cb} + hole^+_{vb}\right)$$

$$H_2O \rightarrow OH^- + H^+$$

Oxidative reaction:

$$hole^+_{vb}OH^-_{ads} \rightarrow {}^{\cdot}OH$$

Table 4 The thermodynamic properties of butadiene interaction on rTiO$_2$-NP by ZINDO/S method

	LnK	ΔS_{ele} (cal/K mol)	ΔH_{ele} (kcal/mol)	ΔG_{ele} (kcal/mol)
Cross bridge of Ti–O(1)				
Butadiene to ethylene	−23,208.08	−1767.22	71.95	9,367,268
Ethylene to CO_2	−6971.00	−858.63	20.51	2,813,642
Cross bridge of Ti–O(2)				
Butadiene to ethylene	−27,951.79	−1357.23	89.24	11,281,928
Ethylene to CO_2	−19,106.49	−1243.95	59.94	7,711,780
Cross bridge of Ti–Ti				
Butadiene to ethylene	−10,476.97	−862.67	32.26	4,228,725
Ethylene to CO_2	−2469.36	−223.22	7.54	996,685.5

$$^{\cdot}OH + \text{Butadiene} \rightarrow 2C_2H_4 + 2H_2$$

$$^{\cdot}OH + 2C_2H_4 + 4O_2 \rightarrow 4CO_2 + 4H_2$$

The results show that the approach and conversion of this interaction are endothermic reaction and for this conversion sunlight (solar energy) or other energies are necessary. As the high temperature (900 °C) of automotive exhaust gases can provide energy for this interaction, in this study, all of the possibilities of interaction between butadiene interaction on rTiO$_2$-NP are investigated, the cross bridge of Ti–O (2) is suitable for converting this interaction. The use of nano-catalysts for the conversion of unburned hydrocarbons (butadiene) to low-risk products is affordable. Dipole moments of rTiO$_2$ structure on the location of Ti–O are more than Ti–Ti, which is related to the electronegativity difference.

References

1. Ogwu, F.A., Peters, A.A., Aliyu, H.B., Abubakar, N.: An Investigative approach on the effect of air pollution on climate change and human health in the niger delta region of Nigeria. Int. J. Sci. Res. Innov. Technol. **2**(5), 37–49 (2015)
2. Razak, M.I.M., Ahmad, H.I., Bujang, I., Talib, A., Ibrahim, Z.: Economics of air pollution in Malaysia. Int. J. Humanit. Soc. Sci. **3**(13), 173–177 (2013)
3. Ahmad Khan, M., Ghouri, A.M.: Environmental pollution: its effects on life and its remedies. J. Arts Sci. Commer. II **2**, 276–285 (2011)
4. Small, K.A., Kazimi, C.: On the costs of air pollution from motor vehicles. J. Transp. Econ. Policy **29**, 7–32 (1995)
5. Naima, K., Liazid, A.: Waste oils as alternative fuel for diesel engine: a review. J Pet Technol Altern Fuels **4**(3), 30–43 (2013)
6. Wang, L., Luo, G.H., Li, Q.: Progress of waste plastics pyrolysis. Chem. Ind. Eng. Progr **22**(2), 130–134 (2003)
7. Air quality control Co. (1997), Tehran transport emission reduction project, part 2–15
8. Heinsohn, R.J., Kabel, R.L.: Sources and control of air pollution, pp. 652–666. Prentice Hall, New Jersey (1999)
9. Cyclone: The 13.4 MW Gas Turbine M. McGurry and B.Igoe (Canadian Gas Association Turbine Symposium, October 2001)
10. Orlandini, I., Riedel, U.: Oxidation of propene and the formation of methyl nitrate in non-thermal plasma discharges. Catal. Today **89**, 83–88 (2004)
11. The Use of Medium Calorific Value gases from Biomass and Municipal Solid Waste in Industrial Gas Turbines M.Welch and P.Martin (CEPSI 2002, Fukuoka, Japan)
12. Martyr, A.J., Plint, M.A.: Engine testing, 3rd edn. Butterworth-Heinetmann, Oxford (2007)
13. Dhage, S.R., Samuel, V.D., Choube, V., Ravi, V.: Synthesis of nanocrystalline TiO2 at 100 °C. Mater. Lett. **58**(17–18), 2310–2313 (2004)
14. Torres, A.R., Azevedo, E.B., Resende, N.S., Dezotti, M.: A comparison between bulk and supported TiO2 photocatalysts in the degradation of formic acid. Braz. J. Chem. Eng. **24**(2), 185–192 (2007)
15. Jones, B.J., Vergne, M.J., Bunk, D.M., Locascio, L.E., Hayes, M.A.: Cleavage of peptides and proteins using light-generated radicals from titanium dioxide. Anal. Chem. **79**(4), 1327–1332 (2007)
16. Earle, M.D.: Electrical conductivity of titanium dioxide. Phys. Rev. **61**(1), 56–62 (1942)
17. Mohamed, R.M., McKinney, D.L., Sigmund, W.M.: Enhanced nanocatalysts. Mater. Sci. Eng. R Rep. **23**(1), 1–13 (2012)
18. Salarvand, A., Mahdavian, L.: Thermodynamic study of dioxin reduced by TiO$_2$ nanoparticles from environment. Energy Environ. Focus **5**(1), 18–22 (2016)
19. Salarvand, A., Mahdavian, L.: Comparison of Ti-Ti and Ti-O bonds in nano-surfaces of rTiO$_2$ (110) for Conversion Dibenzo-dioxine to CO$_2$. Int. Res. J. Appl. Basic Sci. **9**(5), 648–655 (2015)
20. Ridley, J., Zerner, M.: An intermediate neglect of differential overlap technique for spectroscopy: pyrrole and the azines. Theoret. Chim. Acta **32**(2), 111–134 (1973)
21. Zerner, M.C. In: Lipkowitz, K.B., Boyd, D.B. (eds.) Reviews in Computational Chemistry, vol. 2, pp. 313–365. VCH, Wiley, New York (1991)
22. Maier, H.: Chemiker im "Dritten Reich". Die Deutsche Chemische Gesellschaft und der Verein Deutscher Chemiker im NS-Herrschaftsapparat, p. 96. Wiley, Weinheim (2015). ISBN 978-3-527-69134-0
23. Diebold, U.: The surface science of titanium dioxide. Surf. Sci. Rep. **48**, 53–229 (2003)

24. Becke, D.: Density functional thermochemistry. III. The role of exact exchange. J. Chem. Phys. **98**, 5648–5652 (1993)
25. Yang, L.W., Parr, R.G.: Development of the Colle-Salvetti correlation-energy formula into a functional of the electron density. Phys. Rev. B: Condens. Matter. **37**, 785–789 (1988)
26. Ulrike, D.: The surface science of titanium dioxide (PDF). Surf. Sci. Rep. **48**(5–8), 53–229 (2003)
27. Zhang, Z., Fenter, P., Sturchio, N.C., Bedzyk, M.J., Machesky, M.L., Wesolowski, D.J.: Structure of rutile TiO_2 (110) in water and 1 molal Rb^+ at pH 12: inter-relationship among surface charge, interfacial hydration structure, and substrate structural displacements. Surf. Sci. **601**, 1129–1143 (2007)
28. High performance computing research center: http://hpcrc.aut.ac.ir
29. http://www.msg.ameslab.gov/gamess/License_Agreement.html
30. Lee, S. Encyclopedia of chemical processing and design. Taylor & Francis, 2005. ISBN: 0824755634, 9780824755638
31. Varghese, O.K., Paulose, M., LaTempa, T.J., Grimes, A.: Grimes high-rate solar photocatalytic conversion of CO_2 and water vapor to hydrocarbon fuels. Nano Lett. **9**(2), 731–737 (2009)